Temperature Bias and the Primordial Helium Abundance Determination

Antonio Peimbert, Manuel Peimbert, & Valentina Luridiana

Instituto de Astronomía, Universidad Nacional Autónoma de México

ABSTRACT

We study the effect that the temperature structure has on the determination of the primordial helium abundance, Y_p. We provide an equation linking T(O III), the temperature derived from the [O III] lines, and T(He II), the temperature of the He I lines, both for H II regions with O^{++} only and for H II regions where a fraction of O^+ is present. By means of T(He II), which is always smaller than T(O III), we derive the helium abundances of 5 objects with low and very low metallicity (NGC 346, NGC 2363, Haro 29, SBS 0335–052, and I Zw 18); these objects were selected from the literature because they include the 3 low metallicity objects with the best line determinations and the 2 objects with the lowest metallicity. From these abundances we obtain that $Y_p(\mathrm{nHc}) = 0.2356 \pm 0.0020$, a value 0.0088 lower than that derived by using T(O III). We call this determination Y_p(nHc) because the collisional contribution to the Balmer line intensities has not been taken into account. All the recent Y_p determinations in the literature have not taken into account the collisional contribution to the Balmer line intensities. By considering the collisional contribution to the Balmer line intensities of these five objects we derive that $Y_p(+\mathrm{Hc}) = 0.2384 \pm 0.0025$.

Subject headings: galaxies: abundances—galaxies: ISM—H II regions—ISM: abundances ***

1. Introduction

The determination of the pregalactic, or primordial, helium abundance by mass Y_p is paramount for the study of cosmology, the physics of elementary particles, and the chemical evolution of galaxies (e.g. Fields & Olive 1998; Izotov et al. 1999; Peimbert & Torres-Peimbert 1999, and references therein). In this paper we present a new determination of Y_p based on observations of the metal-poor extragalactic H II regions NGC 346, I Zw 18, NGC 2363, Haro 29, and SBS 0335–052. This determination is compared with those carried out by other authors. A preliminary account on the results for I Zw 18 and NGC 2363 is presented elsewhere (Peimbert, Peimbert, & Luridiana 2001).

There are three problems affecting the Y_p determination that need to be further analyzed: *a*) the temperature structure, *b*) the ionization structure, and *c*) the collisional excitation of the hydrogen lines. This paper will be mainly concerned with the effect of the temperature structure of the nebulae on the helium line intensities. In a future paper we will discuss in more detail

the problem of the collisional excitation of the hydrogen lines (Luridiana, Peimbert, & Peimbert 2001). The most accurate Y_p values in the literature have been derived under the assumption of no contribution to the hydrogen Balmer lines due to collisional excitation, we will refer to these determinations in this paper as Y_p(nHc) and to those that include the hydrogen collisional effect as Y_p(+Hc). Due to the collisional contribution to the Balmer line intensities the Y_p(nHc) determinations are lower limits to the Y_p(+Hc) value.

There are several pieces of evidence indicating that T(He II) is smaller than T(O III): *a*) observations of NGC 346 (Peimbert, Peimbert, & Ruiz 2000, hereinafter Paper I), *b*) photoionization models of giant extragalactic H II regions (Stasińska & Schaerer 1999; Luridiana et al. 1999, 2001; Relaño et al. 2001), *c*) in photoionization models T(O II) is smaller than T(O III) for objects with T(O III) higher than 12,360 K (Stasińska 1990), and a considerable fraction of the He I lines originates in the O^+ zone. This small difference is significative because it lowers the He^+/H^+ determination. By combining the observed He I lines it is found that T(He II) and N_e(He II) are coupled in the sense that a lower T implies a higher N_e reducing the He^+/H^+ determination (see Paper I).

Another problem that has to be considered to determine very accurate He/H values of a given H II region is its ionization structure. The total He/H value is given by:

$$\begin{aligned}\frac{N(\mathrm{He})}{N(\mathrm{H})} &= \frac{\int N_e N(\mathrm{He}^0)dV + \int N_e N(\mathrm{He}^+)dV + \int N_e N(\mathrm{He}^{++})dV}{\int N_e N(\mathrm{H}^0)dV + \int N_e N(\mathrm{H}^+)dV}, \\ &= ICF(\mathrm{He})\frac{\int N_e N(\mathrm{He}^+)dV + \int N_e N(\mathrm{He}^{++})dV}{\int N_e N(\mathrm{H}^+)dV}. \end{aligned} \quad (1)$$

For objects of low degree of ionization it is necessary to consider the presence of He^0 inside the H^+ zone, while for objects of high degree of ionization it is necessary to consider the possible presence of H^0 inside the He^+ zone. For objects of low degree of ionization ICF(He) might be larger than 1.00, while for objects of high degree of ionization ICF(He) might be smaller than 1.00. This problem has been discussed by many authors (e.g. Shields 1974; Stasińska 1983; Peña 1986; Vílchez & Pagel 1988; Pagel et al. 1992; Armour et al. 1999; Peimbert & Peimbert 2000; Viegas, Gruenwald, & Steigman 2000; Viegas & Gruenwald 2000; Ballantyne, Ferland, & Martin 2000; Sauer & Jedamzik 2001).

Each H II region is different and a good photoionization model is needed to estimate an ICF(He) of very high accuracy. In this paper we will assume that the H II regions are chemically homogeneous.

In section 2 we will adapt the t^2 and T_0 formalism introduced by Peimbert (1967) to relate T(O III) and T(O II) with T(He II), the full mathematical treatment is presented in the Appendix. In section 3 we will rediscuss the Y determination of NGC 346, the most luminous H II region in the SMC, carried out in Paper I. In sections 4 to 7 we redetermine the He^+/H^+ values for I Zw 18,

NGC 2363, Haro 29, and SBS 0335–052, based on the observations of Izotov, Thuan, & Lipovetsky (1997) and Izotov et al. (1999) and on photoionization models for these objects. These four objects were selected from their sample based on the following criteria: the two objects with the lowest heavy element abundances and the two objects with the smallest observational errors (Peimbert & Peimbert 2001). We derive He^+/H^+, N_e(He II), T(He II), and $\tau(3889)$ self-consistently based on all the observed He I line intensities, with the exception of those strongly affected by underlying absorption. By combining the He^+/H^+ values of these four objects with that of NGC 346 we derive a new Y_p(nHc) in section 8. The collisional contribution to the Balmer lines is estimated in section 9. The discussion and conclusions are presented in sections 10 and 11.

2. Temperatures

2.1. T(O III) and T(He II) for a pure O^{++} nebula

We first consider an H II region where the He II, the O III, and the H II volumes coincide perfectly. If we further assume that the temperature is constant we have a very simple model which gives us a first approximation to a real nebula.

If we now assume that the H II region has an average temperature given by

$$T_0 = \frac{\int T N_e N_p \, dV}{\int N_e N_p \, dV}, \tag{2}$$

and a mean square temperature variation given by:

$$t^2 = \frac{\int (T - T_0)^2 N_e N_p \, dV}{T_0^2 \int N_e N_p \, dV}, \tag{3}$$

we find that the observed $T(4363/5007)$, derived from the $I(4363)/I(5007)$ ratio, is given by (Peimbert 1967):

$$T(\text{O III}) = T_0 \left(1 + \left[\frac{90800}{T_0} - 3\right] \frac{t^2}{2}\right), \tag{4}$$

and that the temperature associated to the He I recombination lines, that originate in the He II region, is (see Paper I):

$$T(\text{He II}) = T_0 \left(1 - 1.4 t^2\right). \tag{5}$$

This means that the temperature that should be used to measure the helium abundance is given by:

$$T(\text{He II}) = T(\text{O III}) \left(1 - \left[\frac{90800}{T(\text{O III})} - 0.2\right] \frac{t^2}{2}\right). \tag{6}$$

In Figure 1, and based on equation 6, we present T(He II)/T(O III) versus t^2 for different values of T(O III).

2.2. T(He II) for a nebula with O$^+$ and O^{++}

We consider now another H II region where the He II volume coincides with the H II volume, but now oxygen is present both in the form of O^{++} and O$^+$, with the O$^+$ weight described by the fraction α:

$$\alpha = \frac{\int N_e N(\mathrm{O}^+)\, dV}{\int N_e N(\mathrm{O}^+)\, dV \, + \, \int N_e N(\mathrm{O}^{++})\, dV}. \tag{7}$$

If the average temperatures in the O II and O III zones are given by:

$$T_{02} = \frac{\int T N_e N(\mathrm{O}^+)\, dV}{\int N_e N(\mathrm{O}^+)\, dV} \tag{8}$$

and

$$T_{03} = \frac{\int T N_e N(\mathrm{O}^{++})\, dV}{\int N_e N(\mathrm{O}^{++})\, dV} \tag{9}$$

respectively, then the average temperature for the whole ionized region T_0 is equal to

$$T_0 = \alpha T_{02} + (1 - \alpha)\, T_{03}; \tag{10}$$

the fractional difference between T_{03} and T_0 can thus be characterized by the parameter β so that

$$\frac{T_{03}}{T_0} = 1 + \beta, \tag{11}$$

and the ratio between T_{02} and T_0 is:

$$\frac{T_{02}}{T_0} = 1 - \beta \left(\frac{1 - \alpha}{\alpha} \right) = 1 + \beta - \frac{\beta}{\alpha}. \tag{12}$$

In the general case when the O II and O III zones are not of uniform temperature, but include temperature fluctuations, represented by:

$$t_2^2 = \frac{\int (T - T_{02})^2 N_e N(\mathrm{O}^+)\, dV}{T_{02}^2 \int N_e N(\mathrm{O}^+)\, dV} \tag{13}$$

and

$$t_3^2 = \frac{\int (T - T_{03})^2 N_e N(\mathrm{O}^{++})\, dV}{T_{03}^2 \int N_e N(\mathrm{O}^{++})\, dV} \tag{14}$$

respectively, the mean square temperature fluctuation for the entire H II region, t^2, is given by:

$$t^2 = \alpha \left(\frac{T_{02} - T_0}{T_0} \right)^2 + (1 - \alpha) \left(\frac{T_{03} - T_0}{T_0} \right)^2 + \alpha t_2^2 \left(\frac{T_{02}}{T_0} \right)^2 + (1 - \alpha)\, t_3^2 \left(\frac{T_{03}}{T_0} \right)^2, \tag{15}$$

were the first two terms represent the deviation from uniform temperature given by the difference in temperature between each zone and the average for the whole H II region, while the other two represent the additional contribution due to inhomogeneities in each zone.

Substituting the first 2 terms with equations 12 and 11 and by keeping the last 2 terms to second order we obtain:

$$\begin{aligned} t^2 &= \alpha\beta^2\left(\frac{1-\alpha}{\alpha}\right)^2 + (1-\alpha)\,\beta^2 + \alpha t_2^2 + (1-\alpha)\,t_3^2 \\ &= \beta^2\left(\frac{1-\alpha}{\alpha}\right) + \alpha t_2^2 + (1-\alpha)\,t_3^2. \end{aligned} \tag{16}$$

T_{03} and t_3^2 are related to $T(\text{O III})$ by (see equation 4):

$$T(\text{O III}) = T_{03}\left(1 + \left[\frac{90800}{T_{03}} - 3\right]\frac{t_3^2}{2}\right); \tag{17}$$

while T_{02} and t_2^2 are related to an O II temperature, determined from the $I(3727)/I(7325)$ ratio, that in the low density limit is given by (Peimbert 1967):

$$T(\text{O II}) = T_{02}\left(1 + \left[\frac{97300}{T_{02}} - 3\right]\frac{t_2^2}{2}\right). \tag{18}$$

It is convenient to obtain an equation, with the same physical meaning than that of equations 17 and 18, that relates T_0 and t^2 with a temperature that can be derived from observations, particularly with those of the O II and O III forbidden lines. Intuitively we can define the following equation (the formal derivation of equation 19 is given in the Appendix):

$$T(\text{O II+III}) = T_0\left(1 + \left[\frac{\theta}{T_0} - 3\right]\frac{t^2}{2}\right), \tag{19}$$

where T_0 and t^2 correspond to the values for the entire volume, θ represents an effective average over the excitation energy needed to produce the oxygen lines,

$$\theta = (1-\alpha)\,90800 + \alpha\,97300 \tag{20}$$

and $T(\text{O II+III})$ is an average between $T(\text{O II})$ and $T(\text{O III})$. However, it can be shown (see Appendix) that, the simple average of the temperatures weighted by α and $1-\alpha$ does not give an equation accurate to second order and that $T(\text{O II+III})$ needs a factor Γ of the form:

$$T(\text{O II+III}) = [(1-\alpha)\,T(\text{O III}) + \alpha\,T(\text{O II})]\,\Gamma, \tag{21}$$

Γ is very close to unity for objects where $\alpha(1-\alpha) < 0.08$ or where $T(\text{O II})$ is similar to $T(\text{O II})$ $(0.9 < T(\text{O II})/T(\text{O III}) < 1.1)$; but for H II regions where there are appreciable fractions of both O^+ and O^{++} and where there is an appreciable difference between $T(\text{O III})$ and $T(\text{O II})$, Γ must be calculated as described in the Appendix. (All computations done in this paper were done using the formalism described in the Appendix.)

Finally, solving equation 19 for T_0 and substituting it in equation 5 it follows that

$$T(\text{He II}) = T(\text{O II+III})\left(1 - \left[\frac{\theta}{T(\text{O II+III})} - 0.2\right]\frac{t^2}{2}\right), \tag{22}$$

which can now be used to determine the He abundances. To derive T(O II+III) from the observed T(O II) and T(O III) values we need to use equations 7, 20, and 21 for $\Gamma = 1$; for Γ larger than one we also need to use equations A2, A3, and A7. If only T(O III) is available we need a photoionization model to obtain a relationship between T(He II) and T(O III).

In Figure 2 we present the relationship between T(He II) and T(O III) as a function of t^2 for objects with different O^+ fractions. Figure 2 is based on equations 7, 20, 21, A2, A3, and A7 and the relationship

$$T_{02} = 2430 + T_{03}(1.031 - T_{03}/54350), \tag{23}$$

derived from the photoionization models by Stasińska (1990). From this equation it is obtained that: for T_{03} = 12,360 K then $T_{03} = T_{02}$, for higher temperatures $T_{03} > T_{02}$, and for lower temperatures $T_{03} < T_{02}$.

From Figure 2 and equation 23 we note the following cases for objects with T(O III) > 12,360 K: *a*) For $\alpha = 0.00$ and ${t_3}^2 = 0.000$, then T(He II) = T(O III) and $t^2 = 0.000$. *b*) For $\alpha \neq 0.00$ and ${t_2}^2 = {t_3}^2 = 0.000$, then T(He II) is *always* smaller than T(O III) and t^2 is *always* larger than 0.000. *c*) For $\alpha = 0.00$, and ${t_3}^2 > 0.000$, then T(He II) < T_e(O III) and $t^2 > 0.000$. *d*) For $\alpha \neq 0.00$ and ${t_2}^2 \sim {t_3}^2 > 0.000$, then T(He II) is even smaller than in case *b* and t^2 is even larger than in case *b*.

Very metal-poor extragalactic H II regions, those that have been used to derive the primordial helium abundance, have T(O III) larger than 12,360 K and are best represented by case *d*.

Figure 2 is also related to the Averaged Quantities block of CLOUDY's output (Ferland 1996; Ferland et al. 1998; Kingdon & Ferland 1995). In that section of CLOUDY's output there is a line labeled "Peimbert" with the following entries: "T(O IIIr)" that corresponds to T(O III) in this paper; "T(Bac)" is the hydrogen temperature resulting from the predicted Balmer jump and Hβ for the optically thick case, corresponds to the outer surface of the object and does not represent typical H II regions; "T(Hth)" is the hydrogen temperature resulting from the predicted Balmer jump and Hβ for the optically thin case, corresponds to T(Bac) defined by Peimbert (1967) and used by many authors, and applies to typical H II regions; "t^2(Hstr)" is the structural value computed across the H II region, and it is called t^2 in this paper. "T(O3-BAC)" and "t^2(O3-BC)" are the average temperature and the mean square temperature fluctuation values derived from the predicted T(O III) and T(Bac) values, they correspond to T_0 and t^2(Hstr) only when all the O is in the O^{++} stage. In the presence of O^+ and according to Figure 2 and equation 23 we can distinguish two cases: when T(O III) is higher than 12,360 K then "t^2(O3-BC)" is higher than t^2, but when T(O III) is smaller than 12,360 K then "t^2(O3-BC)" is smaller than t^2.

From photoionization models of H II regions it has been found that t^2 is in the 0.002 to 0.03 range, with typical values around 0.005 (e.g. Gruenwald & Viegas 1992; Kingdon & Ferland 1995; Pérez 1997); from observations it has been found that t^2 is in the 0.01 to 0.04 range, with typical values around 0.03 (e.g. Peimbert 1995, 1999, and references therein). As a first approximation due to equation 23 we expect minimum t^2 values from photoionized models with $T \sim$ 12,360 K and an increase in t^2 for hotter and cooler models. Most of the observational determinations of t^2

come from H II regions with T(O III) $\sim$ 8000 K which are biased toward one of the higher ends of the t^2 distribution. Very metal-poor H II regions are biased to the other high end of the t^2 distribution, particularly those with WR stars and a large fraction of O^+. The t^2 values derived from photoionization models correspond to T(He II) values 3% to 11% smaller than T(O III). In the presence of additional sources of energy, to those provided by photoionization, the difference between T(He II) and T(O III) might be larger.

3. NGC 346

In Paper I we have analyzed NGC 346, the most luminous H II region in the Small Magellanic Cloud. Due to the relatively small distance to NGC 346 it is possible to place the observing slit avoiding the brightest stars, thus minimizing the effect of the underlying absorption in the He^+/H^+ determination.

The determination of Y_p based on NGC 346 can have at least four significant advantages and one disadvantage with respect to those based on distant H II region complexes: *a*) no underlying absorption correction for the helium lines is needed because the ionizing stars can be excluded from the observing slit, *b*) the determination of the helium ionization correction factor can be estimated by observing different lines of sight, *c*) the accuracy of the determination can be estimated by comparing the results derived from different lines of sight, *d*) the electron temperature is generally smaller than those of metal poorer H II regions reducing the effect of collisional excitation from the metastable 2^3 S level of He I and from the ground level of H I, and *e*) the disadvantage is that the correction due to the chemical evolution of the SMC is in general larger than for the other systems.

From the observations of the He I lines $\lambda\lambda$ 3889, 4026, 4387, 4471, 4922, 5876, 6678, 7065, and 7281 (see Table 1) and from the temperatures associated with the O III lines and the Balmer discontinuity in region A we have used a maximum likelihood method to determine simultaneously and self-consistently several parameters. Our results are: N_e(He II)= 144^{+44}_{-38} cm^{-3}, T(He II)= $11,860 \pm 370$ K, He/H $= 0.07910 \pm 0.00072$, and $\tau(3889) = 0.0$. For this temperature range we obtain that O/H= $(141 \pm 21) \times 10^{-6}$. In Table 2 we present He/H and χ^2 as a function of several N_e(He II) and T(He II) values, which include a few representative temperatures and the densities favored by those temperatures. From this table it can be seen that the minimum χ^2 values imply a strong correlation between the temperature and the density, in the sense that the lower the temperature, the higher the density, and consequently the lower the He/H value. In Paper I it is also found that T_e(He II) is $8.6\% \pm 3\%$ smaller than T_e(O III). The parameters that represent this model are presented in Table 3.

In Table 4 we present the Y(nHc) values for different temperatures and densities, where we have included the He^{++}/H^+ ratio (see Paper I) and an ICF(He) = 1.00.

Relaño et al. (2001) have computed photoionization models for NGC 346 with CLOUDY, they have found: *a*) that there is a negligible amount of H^0 inside the He^+ zone, in agreement with

Paper I, *b*) that T(He II) is 5% smaller than T(O III) in their best model, and *c*) that the T(O III) computed by the models is 9% smaller than the observed value, indicating the presence of additional heating sources not included in the photoionization models and probably implying that the real difference between T(He II) and T(O III) is higher than predicted by the models.

4. I Zw 18

Up to now, with the exception of NGC 346, it has not been possible to derive the ICF(He), N_e(He II), T(He II), $\tau(3889)$, and the He$^+$/H$^+$ ratio based only on the helium lines. Usually the observed T(O III) value has been used to complement the information provided by the He I lines, moreover it has also been assumed that the observed T(O III) is equal to T(He II). For I Zw 18, SBS 0335–052, NGC 2363, and Haro 29 we will make use of the observed T(O III), but we will not assume that it is equal to T(He II), instead we will make use of photoionization models computed with CLOUDY to relate both quantities.

In general photoionization models predict T(O III) values smaller than observed (Stasińska & Schaerer 1999; Luridiana et al. 1999; Luridiana & Peimbert 2001; Luridiana et al. 2001; Relaño et al. 2001) indicating the possible presence of an additional heating source not considered by the models; this result also implies that the T(He II) values predicted by the models will be smaller than those T(He II) values derived from the observed T(O III) values. Since the lower the temperature, the lower the derived He/H value (see for example Table 5), the use of the temperatures predicted by the models yields spuriously low He/H values. On the other hand the models can give us an estimate of t^2(O III), probably a lower limit. The formalism presented in section 2, together with t^2(O III), provides a relationship between the observed T(O III) and T(He II).

From photoionization models of I Zw 18 based on CLOUDY (Luridiana et al. 2001) we find that: $ICF(\mathrm{He}) = 1.00$, $\tau(3889) = 0.010 \pm 0.005$, and t^2(O III)$= 0.013 \pm 0.006$. We consider t^2(O III) as a lower limit to t^2 (see equations 16 and A9). From the formalism of section 2 together with $\alpha = 0.265$ and $T(\mathrm{O\ III}) = 19,060$ K (Izotov et al. 1999) we obtain $t^2 = 0.024 \pm 0.006$ and consequently that T(He II) is 10.2% smaller than T(O III).

To derive the He$^+$/H$^+$ ratio we have used the maximum likelihood method, MLM (see Paper I). The inputs are: *a*) $\tau(3889) = 0.010 \pm 0.005$, *b*) $t^2 = 0.024 \pm 0.006$, *c*) T(O III)$= 19,060$ K and *d*) the observations of $\lambda\lambda$ 3889, 4026, 4471, 5876, 6678, and 7065 by Izotov et al. (1999), where we have adopted the line intensity ratios presented in Table 1, corrected by underlying absorptions of 3.3Å, 0.8Å, and 0.8Å for $\lambda\lambda$ 3889, 4026 and 4471 respectively, that correspond to a burst model of 4 Myr (González-Delgado, Leitherer, & Heckman 1999). The underlying absorptions predicted by the burst model have been reduced by about 10% to take into account the presence of the nebular continuum emission; a similar reduction has been applied to the underlying absorptions predicted by the starburst models for NGC 2363, Haro 29, and SBS 0335–052.

To obtain He$^+$/H$^+$ values we need a set of effective recombination coefficients for the He and H

lines, the contribution due to collisional excitation to the helium line intensities, and an estimate of the optical depth effects for the helium lines. The recombination coefficients that we used were those by Storey & Hummer (1995) for H, and Smits (1996) for He. The He I collisional contribution was estimated from Kingdon & Ferland (1995) and Benjamin, Skillman, & Smits (1999). The optical depth effects in the He I triplet lines were estimated from the computations by Robbins (1968), and based on Paper I we will assume that the He I singlet lines are produced under case B.

The maximum likelihood solution amounts to *a*) N_e(He II)= 87^{+94}_{-78} cm^{-3}, *b*) He$^+$/H$^+$ = 0.07673 ± 0.00312, *c*) $\chi^2 = 4.2$, and *d*) T_e(He II)= $17,120 \pm 600$ K, 10.2% smaller than T(O III) (see Table 3). For this temperature range we obtain that O/H = $(19 \pm 2) \times 10^{-6}$. There is not enough information to independently derive the t^2 and $\tau(3889)$ values from the observed lines in this object, therefore their output values are equal to the input values. Table 5 presents the Y(nHc) values for four t^2 values: 0.024 (the optimum value), 0.030 (+ 1σ), 0.018 (- 1σ), and 0.006 (the minimum possible value given by the size and temperature of the O$^+$ zone); and 6 different densities that include those provided by the MLM for each t^2. The Y(nHc) values include the contribution due to He^{++} and an ICF(He) = 1.00.

5. NGC 2363

The T(O III) values for the four objects observed by Izotov et al. (1997) and Izotov et al. (1999) were derived by us from the observed line intensities, we obtain the same results for I Zw 18 and SBS 0335–052 than Izotov et al. (1999), but we obtain values 650 K higher for NGC 2363 and Haro 29 than Izotov et al. (1997).

Luridiana et al. (1999) produced detailed photoionization models of NGC 2363, they find also that the T(O III) predicted by the models is considerably smaller than 15,750 K, the observed value; from their models they find also that t^2 is in the 0.007 to 0.029 range. This amounts to a T(He II) 6% ± 2% smaller than T(O III). From the models of NGC 2363 and the slit used by Izotov et al. (1997) we also find that: ICF(He) = 0.993, indicating the presence of neutral hydrogen inside the ionized helium region (see equation 1), and $\tau(3889) = 0.50 \pm 0.15$.

Support for the relative high density comes from the N_e[S II] derived by Izotov et al. (1997) and by Esteban et al. (2001) that amount to 120 cm^{-3} and 340 ± 120 cm^{-3} respectively and the N_e [Ar IV] values in the 400 to 800 cm^{-3} range derived by Pérez, González-Delgado, & Vílchez (2001) and the 1300 ± 500 cm^{-3} value derived by Esteban et al. (2001); the [S II] lines trace the outer parts while the [Ar IV] lines trace the inner parts of the H II region.

For the MLM we use the following inputs: *a*) $\tau(3889) = 0.5 \pm 0.3$, *b*) $t^2 = 0.018 \pm 0.011$, *c*) T(O III)= 15,750 K, and *d*) the observations of $\lambda\lambda$ 3820, 3889, 4026, 4387, 4471, 5876, 6678, 7065, and 7281 by Izotov et al. (1997) slightly modified to take into account underlying absorptions of 0.3Å, 1.8Å, 0.4Å, 0.2Å, and 0.4Å for $\lambda\lambda$ 3820, 3889, 4026, 4387, and 4471 respectively (see Table 1), that correspond to a burst model of 3 Myr (González-Delgado et al. 1999). We did not consider

$\lambda 4922$ because its intensity was many σ away from the solution increasing χ^2 to unacceptable values; we also adopted an error for $\lambda 3889$ three times larger than the one given by Izotov et al. (1997) due to our estimate of the combined errors produced by the reddening correction and the underlying absorption correction.

With these inputs we obtain *a*) $N_e(\text{He II}) = 250^{+88}_{-77}$ cm^{-3}, *b*) $t^2 = 0.021 \pm 0.010$, *c*) $\tau(3889) = 0.98 \pm 0.25$, *d*) $\text{He}^+/\text{H}^+ = 0.07997 \pm 0.00153$, *e*) $\chi^2 = 12.9$, and *f*) $T(\text{He II}) = 14,710 \pm 440$ K, a value 6.5% smaller than $T(\text{O III})$ (see Table 3).

Note that the t^2 and $\tau(3889)$ output values are not the same as the input values. This is because the quality of the measurements for NGC 2363 is better than that of I Zw 18, and thus the values of t^2 and $\tau(3889)$ can be directly estimated from the lines, however these values are not as accurate as those of NGC 346 and the error bars would be very large, therefore the observed line intensities get mixed with the t^2 and $\tau(3889)$ input values in the MLM, giving us a different output.

For this temperature distribution we obtain O/H= $(95 \pm 8) \times 10^{-6}$. Table 6 presents the Y(nHc) values for four t^2 values: 0.021 (the optimum value), 0.031 (+ 1σ), 0.011 (- 1σ), and 0.001 (the minimum possible value given by the size and temperature of the O^+ zone); and 6 different densities that include those provided by the MLM for each t^2. The Y(nHc) values include the contribution due to He^{++} and an $ICF(\text{He}) = 0.993$.

6. Haro 29

Haro 29, also known as I ZW 36 or Markarian 209, is one of the two blue compact galaxies with the smallest observational errors in the list of Izotov et al. (1997), the other being NGC 2363.

From photoionization models of Haro 29 based on Cloudy by Luridiana et al. (2001) and the slit used by Izotov et al. (1997) it is again found that the $T(\text{O III})$ values predicted by the models are in the 14,550 to 15,100 K range, values considerably smaller than the observed value of 16,050 K; from these models it is also found that $ICF(\text{He}) = 0.995$ - 0.996, $\tau(3889) \approx 1.4$, and $t^2 = 0.002$ -0.004.

For the MLM we use the following inputs: *a*) $\tau(3889) = 1.43 \pm 0.715$, *b*) $t^2 = 0.020 \pm 0.007$, and *c*) the observations of $\lambda\lambda$ 3820, 3889, 4026, 4387, 4471, 5876, 6678, 7065, and 7281 by Izotov et al. (1997) slightly modified to take into account underlying absorptions of 0.4Å, 2.2Å, 0.6Å, 0.3Å, and 0.6Å for $\lambda\lambda$ 3820, 3889, 4026, 4387, and 4471 respectively (see Table 1), that correspond to a burst model of 3.2 Myr (González-Delgado et al. 1999). We did not consider λ 4922 because its intensity was many σ away from the solution increasing χ^2 to unacceptable values; we also adopted errors for $\lambda\lambda 3889$ and 7065 three and two times larger than the one given by Izotov et al. (1997) due to our estimate of the combined errors produced by the reddening correction and the underlying absorption correction.

From these inputs we obtain: N_e(He II)$= 45^{+77}_{-66}$ cm^{-3}, $\tau(3889) = 0.899 \pm 0.296$, $t^2 = 0.019 \pm 0.007$, and He$^+$/H$^+$ $= 0.08157 \pm 0.00188$. The density result is of great concern, not only is the lower limit unphysical, but the derived value is similar to the root mean square density, $N_e(rms)$, that amounts to $= 47 \pm 7$ cm^{-3}. Giant H II regions usually show $N_{\rm e}(rms)$ values considerably smaller than those densities determined through a forbidden-line ratio or from the He I lines based on the maximum likelihood method, $N_{\rm e}^2(local)$; to quantify the difference the filling factor ϵ is used and is defined by means of the relation:

$$N_{\rm e}^2(rms) = \epsilon N_{\rm e}^2(local). \tag{24}$$

Typical values of ϵ for giant H II regions are in the 0.001 to 0.1 range (e.g. Paper I; Luridiana et al. 1999; Luridiana & Peimbert 2001; Relaño et al. 2001) that would imply a N_e(He II) in the 149 to 1490 cm^{-3} range. Since the density derived from the MLM implies an $\epsilon \approx 1.00$, an unacceptable value, we decided to make another estimate of N_e(He II).

From the CLOUDY models by Luridiana et al. (2001) we found that a good fit to the observed line intensities is obtained with $\epsilon \approx 0.04$, which corresponds to an N_e(He II)$= 235 \pm 85$ cm^{-3}. Fixing this density as our preferred value we obtain $\tau(3889) = 0.41 \pm 0.30$, $t^2 = 0.023 \pm 0.007$ (see Table 3), and He$^+$/H$^+$ $= 0.07800 \pm 0.00178$, other values can be obtained or interpolated from Table 7. The Y(nHc) values include the contribution due to He^{++} and an ICF(He) $= 0.995$.

For this temperature distribution we obtain O/H$= (78 \pm 10) \times 10^{-6}$.

7. SBS 0335–052

After I Zw 18, SBS 0335–052 is the extragalactic H II region with the second lowest metallicity known; and being brighter than I Zw 18 makes it critical in determining Y_p.

We have computed a series of CLOUDY models for SBS 0335–052 (Luridiana et al. 2001). We find that the T(O III) predicted by the models is T(O III) = 17,500 - 18,500 K, again considerably smaller than the observed value of 20,500 K. For the three central values of the observing slit used by Izotov et al. (1999) (center, 0.”6SW, 0.”6NE) we have extracted from the models the following predictions: ICF(He) $= 0.9985$, $\tau(3889) \approx 1.26$, and t^2 in the 0.010 to 0.015 range.

To correct for underlying absorption the blue helium lines and the Balmer lines observed by Izotov et al. (1999) we adopted the values predicted by González-Delgado et al. (1999) for a 3 Myr old instantaneous burst with $Z = 0.001$. The corrections for $\lambda\lambda$ 4026, 4471, 4922, 3889 and Hβ amount to 0.4Å, 0.4Å 0.3Å 1.8Å and 2.0Å respectively. Note that Izotov et al. (1999) corrected the Balmer lines for an underlying absorption of 0.2Å and that they did not correct the helium lines. We adopted the C(Hβ) value determined by Izotov et al. (1999) that is mainly based on the I(Hα)/I(Hβ) ratio, this ratio is not affected by underlying absorption (but it might be affected by collisional excitation of the Balmer lines, see below). The line ratios are presented in Table 1.

From the MLM and the following inputs: *a* $\tau(3889) = 1.26 \pm 0.63$, *b*) $t^2 = 0.020 \pm 0.007$, and *c*) the modified observations of $\lambda\lambda$ 3889, 4026, 4471, 5876, 6678, and 7065 (λ 4922 was not considered because its intensity was many σ away from the solution increasing the χ^2 to unacceptable values); we obtain N_e(He II)= 297^{+65}_{-56} cm^{-3}, He$^+$/H$^+$ $= 0.07640 \pm 0.00152$, $\tau(3889) = 1.60 \pm 0.35$, and $t^2 = 0.021 \pm 0.007$, this t^2 corresponds to a T(He II) $= 19,290 \pm 310$ K (see Table 3).

For this temperature distribution we obtain O/H= $(24 \pm 3) \times 10^{-6}$. Table 8 presents the Y(nHc) values for four t^2 values: 0.021 (the optimum value), 0.028 (+ 1σ), 0.014 (- 1σ), and 0.004 (the minimum possible value given by the size and temperature of the O$^+$ zone); and 6 different densities that include those provided by the MLM for each t^2. The Y(nHc) values include the contribution due to He^{++} and an ICF(He) = 0.9985.

8. Determination of Y_p(nHc)

In Table 9 we compare the Y(nHc) maximum likelihood values computed in this paper for $t^2 \neq 0.000$ (see Tables 4-8) with the Y(nHc) values for $t^2 = 0.000$ computed by Izotov et al. (1997, 1999). The differences in the Y values between both types of determinations are of the order of 0.0070, and are manly due to the treatment of the temperature. The errors that we quote are larger than those by Izotov and colaborators, both groups include the errors in the observed line intensity ratios, however we also include the uncertanties on the N_e(He II), t^2, and $\tau(3889)$ values while they do not. None of the Y(nHc) errors include the uncertanties due to the collisional excitation of the Balmer lines (which will be discussed in the next section) nor the prescence of other possible systematic effects. In Figure 3 we also present the Y(nHc) versus O/H diagram for all the objects.

To determine the Y_p(nHc) value for all the objects it is necessary to estimate the fraction of helium present in the interstellar medium produced by galactic chemical evolution. We will assume that

$$Y_p = Y - O\frac{\Delta Y}{\Delta O}, \tag{25}$$

where O is the oxygen abundance by mass. The ΔO baseline given by the five objects in the sample is very small and consequently produces large errors in the $\Delta Y/\Delta O$ determination, therefore we decided to adopt $\Delta Y/\Delta O = 3.5 \pm 0.9$, the slope derived in Paper I. From this slope and the five Y(nHc) values for $t^2 \neq 0.000$ presented in Table 9 we derive Y_p(nHc)= 0.2356 ± 0.0020. In Table 9 we present the Y_p(nHc) determination derived from the Y(nHc) values for $t^2 = 0.000$ obtained by Izotov & Thuan (1998) and Izotov et al. (1999) for Haro 29, NGC 2363, I Zw 18, and SBS 0335–052, and find that our result is 0.0088 smaller than theirs. The main difference is due to our use of T(He II) instead of T(O III) used by them.

9. Collisional excitation of the hydrogen lines

Davidson & Kinman (1985) were the first to estimate the collisional contribution to the Balmer lines and its effect on the determination of Y_p; they made a crude estimate of this effect for I Zw 18 and concluded that the contribution to $I(\mathrm{H}\alpha)$ *may* be roughly 2%. All the subsequent determinations of Y_p in the literature have been derived under the assumption of no contribution to the hydrogen Balmer lines due to collisional excitation, we have referred to these determinations in this paper as Y_p(nHc) and as Y_p(+Hc) to those primordial helium abundance determinations that include the collisional contribution effect. Further discussion of the relevance of the collisional contribution to the Balmer lines is presented elsewhere (Stasińska & Izotov 2001; Luridiana et al. 2001).

From observations it is not easy to estimate this effect for two reasons: small changes are expected in the Balmer line ratios, and the increase in $I(\mathrm{H}\alpha)/I(\mathrm{H}\beta)$ due to collisions can be ascribed to a spuriously higher $C(\mathrm{H}\beta)$. The He/H line ratios are affected by the increase of the Balmer line intensities due to collisions and by the decrease of $C(\mathrm{H}\beta)$ due to the increase of $I(\mathrm{H}\alpha)/I(\mathrm{H}\beta)$.

From a series of Cloudy models it is found that the collisional contribution to $I(\mathrm{H}\beta)$ for I Zw 18 and SBS 0335–052 is in the 2% to 6% range, for Haro 29 and NGC 2363 in the 1% to 3% range and for NGC 346 in the 0.6% to 1.2% range. The effect of collisions on the Balmer line intensities together with the Cloudy models for I Zw 18, SBS 0335–052, and Haro 29 will be discussed extensively elsewhere (Luridiana et al. 2001). The Cloudy models for NGC 2363 and NGC 346 are those by Luridiana et al. (1999) and Relaño et al. (2001) respectively.

To estimate Y(+Hc) for NGC 346, NGC 2363, Haro 29, and I Zw 18 we used the published Balmer line intensities without modifying the $C(\mathrm{H}\beta)$ determination, the reason is that the published $C(\mathrm{H}\beta)$ values are already very low and do not seem to indicate that they have been overestimated. For NGC 346 the published $C(\mathrm{H}\beta)$ value is 0.15±0.01 and the value derived from the embedded stellar cluster amounts to 0.19 ± 0.01 (see Paper I), for NGC 2363 and Haro 29 $C(\mathrm{H}\beta)$ amounts to 0.11 and 0.00 respectively (Izotov et al. 1997), and for I Zw 18 it amounts to 0.015 ± 0.020 (Izotov et al. 1999). The Y(+Hc) estimates are presented in Table 9, where the collisional contribution was obtained from the models mentioned in the previous paragraph. The errors in the Y(+Hc) determinations include the same errors as the Y(nHc) determinations plus the error produced by the uncertainty in the collisional contribution effect, but they do not include the errors due to other possible systematic effects.

Alternatively Izotov et al. (1999) derived for the three central positions of SBS 0335–052 a $C(\mathrm{H}\beta)$ value of 0.237 ± 0.019, but the value derived from $I(\mathrm{H}\alpha)/I(\mathrm{H}\beta)$ is higher than those derived from $I(\mathrm{H}\gamma)/I(\mathrm{H}\beta)$ and $I(\mathrm{H}\delta)/I(\mathrm{H}\beta)$ (after correcting the Balmer lines for underlying absorption as mentioned in section 7); this difference could be due to collisional excitation of the Balmer lines, therefore from the corrected Balmer lines for underlying absorption and from the effect of collisions, as predicted by one of our Cloudy models, we obtained a $C(\mathrm{H}\beta)$ of 0.15; for this value of the reddening we corrected all the line intensities and from them we derived the Y(+Hc) value

presented in Table 9.

Our preliminary result of Y_p(+Hc), is about 0.0028 larger than Y_p(nHc) (see Table 9). From Table 9 it can be seen that the Y(+Hc) values for NGC 346, NGC 2363 and Haro 29 are similar to those for I Zw 18 and SBS 0335–052. This result *may* indicate that the corrections adopted for collisional excitation of the Balmer lines have been overestimated because the production of helium due to galactic chemical evolution is expected to be higher for the first three objects than for the last two (see equation 25).

10. Discussion

The brightest extragalactic H II regions with temperatures in the 14,000 to 16,000 K range might be the best objects to determine Y_p. The reasons are the following: *a*) there are many of these objects available and the brightest of them are brighter than the metal-poorest objects known which implies that the errors in the line intensity ratios will be smaller, and *b*) the effect of collisional excitation of the Balmer lines is considerably smaller than for the metal-poorer objects (those with temperatures in the 18,000 to 22,000 K range) reducing the error in the Y determination due to this effect.

On the other hand the correction to the Y determination to obtain Y_p based on objects with temperatures in the 14,000 to 16,000 K range increases the error in the Y_p determination, but in general the size of this error is expected to be smaller than those introduced in the previous paragraph because the correction is small and can be obtained with high accuracy under the assumption that $\Delta Y/\Delta O = 3.5 \pm 0.9$ (see Paper I). From chemical evolution models it is found that changes in $\Delta Y/\Delta O$ are small even in the presence of a very strong burst of star formation (Carigi, Colín, & Peimbert 1999); moreover these objects seem to have been forming stars over periods of at least 1 to 2 Gyr implying that most of their oxygen formed before the present burst, as in the case of Haro 29 (e.g. Schulte-Ladbeck et al. 2001), and consequently that the expected changes in $\Delta Y/\Delta O$ due to bursts are very small.

The Y_p(nHc) value derived by us is significantly smaller than the value derived by Izotov & Thuan (1998), from the Y – O/H linear regression for a sample of 45 BCGs, and by Izotov et al. (1999), from the average for the two most metal deficient galaxies known (I Zw 18 and SBS 0335–052), that amount to 0.2443 ± 0.0015 and 0.2452 ± 0.0015 respectively.

Our T_e(He II) determinations, that we prefer, produce Y values that are about 0.007 smaller than those derived by Izotov & Thuan (1998) and Izotov et al. (1999), a small but significative difference, as we will see below. It should be noted that the abundances for NGC 2363, SBS 0335–052, Haro 29, and I Zw 18 obtained by both groups are based on the same observations.

From photoionization models computed with CLOUDY we estimate that T(He II), the temperature that should be used to determine the helium abundance, should be at least 5% smaller than

T(O III). Moreover, if in addition to photoionization there is additional energy injected to the H II region the difference between T(O III) and T(He II) might be even larger.

Figure 4 shows the helium, deuterium, and lithium abundances predicted by standard Big Bang nucleosynthesis computations with three light neutrino species for different values of η, the baryon to photon ratio (Thomas et al. 1994; Fiorentini et al. 1998), also in this figure we present observational abundance determinations of these elements. The implications of this figure for the determination of Ω_b, the baryon content of the Universe, are presented in Table 10.

11. Conclusions

Based on the best observations of extragalactic H II regions of low metallicity available in the literature we redetermine the primordial helium abundance, Y_p(nHc), taking into account all the observed He I line intensities with the exception of those strongly affected by underlying absorption. We derive He/H, N_e(He II), T(He II), and $\tau(3889)$ self-consistently.

From the same data for NGC 2363, SBS 0335–052, Haro 29, and I Zw 18 we obtain Y(nHc) values about 0.007 smaller than those derived by Izotov, Thuan and collaborators, the differences are small but significant and are mainly due to the lower T(He II) values adopted by us. In the self-consistent solutions the lower T(He II) values imply higher densities; the higher the density, the higher the collisional contribution to the He I line intensities and consequently the lower the helium abundances (see Tables 2 and 4-8). The Y_p(nHc) value derived by us from NGC 346, NGC 2363, SBS 0335–052, Haro 29, and I Zw 18 is in good agreement with that derived from NGC 346 in Paper I.

The Y(nHc) values are lower limits to the real Y values because they do not consider the excitation of the Balmer lines due to collisions. A preliminary estimate of Y(+Hc) is presented in Table 9. In a future paper we will give a full discussion of this problem (Luridiana et al. 2001) based on detailed models for each object.

The Y_p(nHc) of $0.2356 \pm 0.0020(1\sigma)$ combined with standard Big Bang nucleosynthesis computations (Thomas et al. 1994; Fiorentini et al. 1998) implies that, at the 2σ confidence level, Ω_b is in the 0.011 to 0.020 range for $h = 0.7$ (see Table 10). Also in Table 10 we present seven other determinations of Ω_b not based on Y_p, our result is in good agreement with five of them, those based on: the primordial Lithium determination, Li$_p$, the Cosmic Background Imager, the baryon budget in the galactic vicinity ($z = 0$), the baryon budget at $z \sim 3.00$ and that derived under the assumption of a flat universe, the SNIa magnitude redshift data to derive Ω_M, and a baryon fraction estimate based on X-ray observations of rich clusters of galaxies (this determination is labeled SNIa in Table 10); on the other hand our result is in disagreement with two of them, those based on: the primordial deuterium determination, D$_p$, and BOOMERANG.

Our Y_p(+Hc) value of 0.2384 ± 0.0025 is also in good agreement with the five determinations

of Ω_b mentioned above and is closer than the Y_p(nHc) value to the other two determinations but still in disagreement with them.

The errors in all determinations need to be reduced to constrain even further the domain available to non standard BBN models.

It is a pleasure to acknowledge several fruitful discussions with: G. Ferland, B. E. J. Pagel, E. Skillman, G. Stasińska, G. Steigman, S. Torres-Peimbert, and S. Viegas.

A. Second order approximation to the two temperature scheme

In this appendix we prove the validity of equation 19. To do this, we need to give a physical meaning to T(O II+III) and consequently to Γ, presented in equation 21. Therefore we need to derive the functional form of Γ that will make equation 19 accurate to second order.

Equation 4 is designed (and by analogy 17 and 18) to take into account the increase in emissivity of the forbidden O III lines with increasing temperature, therefore giving higher $T(\text{O III}) - T_0$ differences to regions with larger temperature fluctuations. We want to give the same physical meaning to equation 19, thus we want the $T(\text{O II+III}) - T_0$ difference to increase with t^2.

This can be physically explained by examining equation 16 where the three terms are positive and thus increase t^2. The first term is related to the temperature difference between the O II and O III zones and the last two terms are related to the temperature fluctuations in each zone. The fluctuations associated with the last two terms correspond to the $T(\text{O II}) - T_{02}$ and $T(\text{O III}) - T_{03}$ Gw3o3h)W differences, therefore by adopting a T(O II+III) of the form $(\alpha)T(\text{O II}) + (1-\alpha)T(\text{O III})$ the fluctuations will produce a $T(\text{O II+III}) - T_0$ difference. The first term should also contribute to the $T(\text{O II+III}) - T_0$ difference, but since this term does not represent a change in t_2^2 or t_3^2, T(O II) and T(O III) will not change either, consequently another term is needed in the definition of T(O II+III) This effect is introduced by multiplying the direct average by a factor Γ, which represents the second order correction due to the difference in temperature between the O II and O III zones, thus T(O II+III) will be of the form:

$$T(\text{O II+III}) = [(1-\alpha)\,T(\text{O III}) + \alpha T(\text{O II})]\,\Gamma, \tag{A1}$$

where

$$\Gamma = 1 + \delta^2 \gamma. \tag{A2}$$

Here δ is the relative difference between T(O II) and T(O III) and γ represents a (free) parameter which will permit to recover the physical meaning of equations 17 and 18. Thus δ is given by

$$\delta = \frac{T(\text{O III})}{T(\text{O II})} - 1. \tag{A3}$$

To have a second order correction in β it is enough to determine δ to first order; to first order $T(\text{O III}) = T_{03}$ and $T(\text{O II}) = T_{02}$, therefore

$$\delta = \frac{\beta}{\alpha}. \tag{A4}$$

Substituting equations 17 and 18 into equation A1 we obtain

$$\begin{aligned}
\frac{T(\text{O II+III})}{T_0} &= \Gamma\left[(1-\alpha)(1+\beta)\left(1-3\frac{t_3^2}{2}\right)+(1-\alpha)\frac{90800}{T_0}\frac{t_3^2}{2}\right.\\
&\quad \left.+\alpha\left(1+\beta-\frac{\beta}{\alpha}\right)\left(1-3\frac{t_2^2}{2}\right)+\alpha\frac{97300}{T_0}\frac{t_2^2}{2}\right]\\
&= \Gamma\left[1-3\left((1-\alpha)\frac{t_3^2}{2}+\alpha\frac{t_2^2}{2}\right)\right.\\
&\quad \left.+\frac{1}{T_0}\left((1-\alpha)\,90800\frac{t_3^2}{2}+\alpha 97300\frac{t_2^2}{2}\right)\right];
\end{aligned} \tag{A5}$$

substituting Γ and keeping this equation accurate to second order in the temperature variations (β, t_2, t_3, and t) we obtain

$$\begin{aligned}
\frac{T(\text{O II+III})}{T_0} &= 1+\delta^2\gamma\\
&\quad -3\left((1-\alpha)\,t_3^2+\alpha t_2^2\right)\frac{1}{2}\\
&\quad +\frac{1}{T_0}\left((1-\alpha)\,90800t_3^2+\alpha 97300t_2^2\right)\frac{1}{2}.
\end{aligned} \tag{A6}$$

To simplify this equation and recover the physical meaning of equation 4 it is necessary for γ to be

$$\gamma = \frac{1}{2}(1-\alpha)\,\alpha\left(\frac{\theta}{T_0}-3\right), \tag{A7}$$

here it is enough to derive γ to zeroth order, so dividing θ by any one of the available temperatures (T_0, T_{02}, T_{03}, $T(\text{O II})$ or $T(\text{O III})$) would be approximately right, thus we obtain

$$\begin{aligned}
\frac{T(\text{O II+III})}{T_0} &= 1-3\left((1-\alpha)\,t_3^2+\alpha t_2^2+\beta^2\frac{1-\alpha}{\alpha}\right)\frac{1}{2}\\
&\quad +\frac{90800}{T_0}(1-\alpha)\left(t_3^2+\beta^2\frac{1-\alpha}{\alpha}\right)\frac{1}{2}\\
&\quad +\frac{97300}{T_0}\alpha\left(t_2^2+\beta^2\frac{1-\alpha}{\alpha}\right)\frac{1}{2}.
\end{aligned} \tag{A8}$$

Under the assumption that

$$t_2^2 \approx t_3^2, \tag{A9}$$

equation 16 becomes

$$t^2 = t_2^2 + \beta^2 \frac{1-\alpha}{\alpha}, \tag{A10}$$

and finally equation A8 becomes

$$T(\text{O II+III}) = T_0 \left(1 + \left[\frac{\theta}{T_0} - 3\right] \frac{t^2}{2}\right), \tag{A11}$$

or

$$T_0 = T(\text{O II+III}) \left(1 - \left[\frac{\theta}{T(\text{O II+III})} - 3\right] \frac{t^2}{2}\right). \tag{A12}$$

Equation A12 can now be combined with those equations that relate T_0 and t^2, to some observable temperature like T(Bac) or T(He II).

To adopt a value of $\Gamma = 1$ in equation 21 is equivalent to assume that the first term in equation 16 is equal to zero. We have already mentioned the parameter space where it is a good approximation to assume $\Gamma = 1$. To obtain very accurate He/H values the exact value of Γ, that includes the second order effects implied by t^2, should be used.

REFERENCES

Armour, M. H., Ballantyne, D. R., Ferland, G. F., Karr, J, & Martin, P.G. 1999, PASP, 111, 1251

Ballantyne, D. R., Ferland, G. J., & Martin, P. G. 2000, ApJ, 536, 773

Benjamin, R. A., Skillman, E. D., & Smits, D. P. 1999, ApJ, 514, 307

Carigi, L., Colín, P., & Peimbert, M. 1999, ApJ, 514, 787

Davidson, K., & Kinman, T. D. 1985, ApJS, 58, 321

Esteban, C., Peimbert, M., Torres-Peimbert, S., & Rodríguez, M. 2001, in preparation

Ferland, G. J. 1996, Hazy, a Brief Introduction to Cloudy, Univ. of Kentucky Dept. of Phys. & Astron. Internal Report

Ferland, G. J., Korista, K. T., Verner, D. A., Ferguson, J. W., Kingdon, J. B., & Verner, E. M. 1998, PASP, 110, 761

Fields, B. D., & Olive, K. A. 1998, ApJ, 506, 177

Fiorentini, G., Lisi, S., Sarkar, S. & Villante, F. L. 1998, Phys. Rev.D, 58, 063506

Fukugita, M., Hogan, C. J., & Peebles, P. J. E. 1998, ApJ, 503, 518

González-Delgado, R. M., Leitherer, C., & Heckman, T. M. 1999, ApJS, 125, 489

Gruenwald, R.B., & Viegas, S.M. 1992, ApJS, 78, 153

Izotov, Y. I., Chaffee, F. H., Foltz, C. B., Green, R. F., Guseva, N. G., & Thuan, T. X. 1999, ApJ, 527, 757

Izotov, Y. I. & Thuan, T. X. 1998, ApJ, 500, 188

Izotov, Y. I., Thuan, T. X., & Lipovetsky, V. A. 1997, ApJS, 108, 1

Kingdon, J., & Ferland, G. 1995, ApJ, 442, 714

Luridiana, V., & Peimbert, M. 2001, ApJ, 553, 663

Luridiana, V., Peimbert, M., & Leitherer, C. 1999, ApJ, 527, 110

Luridiana, V., Peimbert, A., & Peimbert, M. 2001, in preparation

Netterfield, C. B., et al. 2001, preprint (astro-ph/0104460)

O'Meara, J. M., Tytler, D., Kirkman, D., Suzuki, N., Prochaska, J. X., Lubin, D., & Wolfe, A. M. 2001, ApJ, 552, 718

Padin, S., et al. 2001, ApJ, 549, L1

Pagel, B. E. J., Simonson, E. A., Terlevich, R. J., & Edmunds, M. G. 1992, MNRAS, 255, 325

Peimbert, A., & Peimbert, M. 2001, in preparation

Peimbert, A., Peimbert, M., & Luridiana, V. 2001, Rev. Mexicana Astron. Astrofis. (Ser. de Conf.), 10, 148

Peimbert, M. 1967, ApJ, 150, 825

Peimbert, M. 1995, in The Analysis of Emission Lines, ed. R.E. Williams & M. Livio (Cambridge: Cambridge University Press), 165

Peimbert, M. 1999, Chemical Evolution from Zero to High Redshift, ed. J. Walsh & M. Rosa, (European Southern Observatory, Springer-Verlag), 30

Peimbert, M., & Peimbert, A. 2000, in IAU Symp. 198, The Light Elements and their Evolution, ed. L. da Silva, M. Spite & J. R. de Medeiros (San Francisco: ASP), 194

Peimbert, M., Peimbert, A., & Ruiz, M. T. 2000, ApJ, 541, 688, Paper I

Peimbert, M., & Torres-Peimbert, S. 1999, ApJ, 525 (Part 3, Centennial Issue), 1143

Peña, M. 1986, PASP, 98, 1061

Pérez, E. 1997, MNRAS, 290, 465

Pérez, E., González-Delgado, R. M., & Vílchez, J. 2001, Ap. & Sp. Sci., in press

Relaño, M., Peimbert, M., & Beckman, J. 2001, ApJ, submitted

Robbins, R. R. 1968, ApJ, 151, 511

Sauer, D., & Jedamzik, K. 2001, A&A, submitted (astro-ph/0104392)

Schulte-Ladbeck, R. E., Hopp, U., Greggio, L., Crone, M. M., & Drozdovsky, I. O. 2001, AJ, 121, 3007

Shields, G. A. 1974, ApJ, 191, 309

Smits, D. P. 1996, MNRAS, 278, 683

Stasińska, G. 1983, in ESO Workshop on Primordial Helium, ed. P. A. Shaver, D. Kunth & K. Kjar (Garching:ESO), p. 255

Stasińska, G. 1990, A&AS, 83, 501

Stasińska, G., & Izotov, Y. I. 2001, A&A, submitted

Stasińska, G., & Schaerer, D. 1999, A&A, 351, 72

Steigman, G., Kneller, J. P., & Zentner, A. 2001 Rev. Mexicana Astron. Astrofis. (Ser. de Conf.), in press (astro-ph/0102152)

Storey, P. J., & Hummer, D. G. 1995, MNRAS, 272, 41

Suzuki, T.K., Yoshii, Y., & Beers, T.C. 2000, ApJ, 540, 99

Thomas, D., Schramm, D. N., Olive, K. A., Mathews, G. J., Meyer, B. S., & Fields, B. D. 1994, ApJ, 430, 291

Viegas, S. M., Gruenwald, R., & Steigman, G. 2000, ApJ, 531, 813

Viegas, S. M., & Gruenwald, R. 2000, in IAU Symp. 198, The Light Elements and Their Evolution, ed. L. da Silva, M. Spite & J. R. de Medeiros (San Francisco:ASP), 188

Vílchez, J. M., & Pagel, B. E. J. 1988, MNRAS, 231, 257

This preprint was prepared with the AAS LATEX macros v5.0.

Table 1. Adopted He I line intensities relative to Hβ

He I line	NGC 346	I Zw 18	NGC 2363	Haro 29	SBS 0335 − 052
3820	...	...	0.012±0.001[c]	0.010±0.001[c]	...
3889[a]	0.0940±0.0017[b]	0.0898±0.0071[c]	0.087±0.001[c]	0.095±0.001[c]	0.0924±0.0028[c,f]
4026	0.0185±0.0007[b]	0.0202±0.0036[c]	0.018±0.001[c]	0.020±0.001[c]	0.0173±0.0006[c,f]
4387	0.0047±0.0002[b]	...	0.005±0.001[c]	0.005±0.001[c]	...
4471	0.0384±0.0005[b]	0.0387±0.0025[c]	0.040±0.001[c]	0.039±0.001[c]	0.0382±0.0007[c,f]
4922	0.0100±0.0002[b]	...	0.013±0.001[c]	...[e]	0.0093±0.0004[c,f]
5876	0.1064±0.0012[b]	0.0936±0.0028[d]	0.106±0.001[d]	0.102±0.001[d]	0.1027±0.0017[f]
6678	0.0296±0.0002[b]	0.0263±0.0018[d]	0.029±0.001[d]	0.029±0.001[d]	0.0263±0.0006[f]
7065	0.0211±0.0002[b]	0.0239±0.0016[d]	0.029±0.001[d]	0.024±0.001[d]	0.0358±0.0007[f]
7281	0.0063±0.0003[b]	...	0.006±0.001[d]	0.005±0.001[d]	...

[a]Where the contribution due to the H8 line has been subtracted.

[b]From Peimbert et al. (2000).

[c]From Izotov et al. (1997, 1999), but modified due to underlying absorption, see text.

[d]From Izotov et al. (1997, 1999).

[e]Presented by Izotov et al. (1997), but not used, see text.

[f]Modified by assuming a different Hβ underlying absorption from that used by Izotov et al. (1999), see text.

Table 2. $N(\mathrm{He}^+)/N(\mathrm{H}^+)$[a] and χ^2 for Region A

t^2	T(He II) (K)	N_e(He II) (cm^{-3}) 69	90	110	144	182	220
0.001[b]	12,800	8052	8014	7980	7924	7865	7810
		(12.4)[c]	(14.0)	(18.4)	(31.7)	(54.2)	(83.3)
0.014	12,240	8036	8001	7969	7917	7861	7809
		(13.0)	(8.81)	(7.53)[c]	(10.8)	(21.7)	(39.0)
0.022	11,860	8026	7992	7961	7911	7858	7808
		(22.3)	(14.5)	(9.58)	(6.53)[c,d]	(10.0)	(19.8)
0.030	11,480	8015	7983	7953	7906	7855	7807
		(39.0)	(27.9)	(19.7)	(10.8)	(7.53)[c]	(10.3)

[a]Given in units of 10^{-5}, for the case of no hydrogen collisions, χ^2 values in parenthesis.

[b]Minimum t^2 value, assuming that ${t_2}^2 = {t_3}^2 = 0.000$ and considering the difference between T_{02} and T_{03}, see text.

[c]The minimum χ^2 value at a given t^2.

[d]The smallest χ^2 value for all t^2's and densities, thus defining T(He II) and N_e(He II).

Table 3. Parameters of the preferred model for each H II region.

Parameter	NGC 346	I Zw 18	NGC 2363	Haro 29	SBS 0335 − 052
T(O III)[a]	13070 ± 50	19060 ± 610	15750 ± 100	16050 ± 100	20500 ± 200
T(He II)[b]	11860 ± 370	17120 ± 600	14710 ± 440	14880 ± 300	19290 ± 310
t^2[b]	0.022 ± 0.008	0.024 ± 0.006	0.021 ± 0.010	0.023 ± 0.007	0.021 ± 0.007
N(He II)[b]	144^{+44}_{-38}	87^{+94}_{-78}	250^{+88}_{-77}	235 ± 85[c]	297^{+65}_{-56}
$\tau(3889)$[b]	0.000	0.010 ± 0.005	0.98 ± 0.25	0.41 ± 0.30	1.60 ± 0.35
ICF(He)[c]	1.000	1.000	0.993	0.995	0.9985

[a]Observed value.

[b]Output from the MLM fit, see text.

[c]From photoionization models, see text.

Table 4. Y(nHc) values for NGC 346

	T(He II)	N_e(He II) (cm^{-3})					
t^2	(K)	69	90	110	144	182	220
0.001[a]	12,800	0.2436[b]	0.2428	0.2420	0.2407	0.2393	0.2381
0.014	12,240	0.2433	0.2425	0.2417[b]	0.2405	0.2392	0.2380
0.022	11,860	0.2430	0.2423	0.2415	0.2404[b,c]	0.2392	0.2380
0.030	11,480	0.2428	0.2420	0.2414	0.2403	0.2391[b]	0.2380

[a]Minimum t^2 value, assuming that ${t_2}^2 = {t_3}^2 = 0.000$ and considering the difference between T_{02} and T_{03}, see text.

[b]Minimum χ^2 value at a given t^2, see Table 2.

[c]The smallest χ^2 value for this object, see Table 2.

Table 5. Y(nHc) values for I Zw 18

		N_e(He II) (cm^{-3})					
t^2	T(He II) (K)	25	59	77	87	97	150
0.006[a]	17,920	0.2404	0.2375[b]	0.2362	0.2354	0.2346	0.2307
0.018	17,390	0.2400	0.2373	0.2359[b]	0.2351	0.2344	0.2307
0.024	17,120	0.2398	0.2371	0.2358	0.2350[b,c]	0.2343	0.2307
0.030	16,860	0.2396	0.2370	0.2357	0.2349	0.2342[b]	0.2307

[a]Minimum t^2 value, assuming that ${t_2}^2 = {t_3}^2 = 0.000$ and considering the difference between T_{02} and T_{03}, see text.

[b]Minimum χ^2 value at a given t^2.

[c]Best fit (minimum χ^2 value) for this object.

Table 6. Y(nHc) values for NGC 2363

	T(He II)	N_e(He II) (cm^{-3})					
t^2	(K)	100	183	214	250	289	338
0.001[a]	15,620	0.2500	0.2459[b]	0.2445	0.2430	0.2414	0.2395
0.011	15,160	0.2493	0.2455	0.2442[b]	0.2427	0.2412	0.2394
0.021	14,710	0.2487	0.2451	0.2438	0.2424[b,c]	0.2410	0.2393
0.031	14,260	0.2480	0.2446	0.2434	0.2421	0.2407[b]	0.2391

[a]Minimum t^2 value, assuming that ${t_2}^2 = {t_3}^2 = 0.000$ and considering the difference between T_{02} and T_{03}, see text.

[b]Minimum χ^2 value at a given t^2.

[c]Best fit (minimum χ^2 value) for this object.

Table 7. Y(nHc) values for Haro 29

	T(He II)	N_e(He II) (cm^{-3})					
t^2	(K)	50	100	150	235	320	500
0.001[a]	15,860	0.2477	0.2451	0.2427	0.2390	0.2356	0.2296
0.016	15,190	0.2471	0.2446	0.2424	0.2389	0.2356	0.2200
0.023	14,880	0.2468	0.2444	0.2422	0.2388[b]	0.2356	0.2302
0.030	14,570	0.2465	0.2441	0.2421	0.2388	0.2356	0.2304

[a]Minimum t^2 value, assuming that ${t_2}^2 = {t_3}^2 = 0.000$ and considering the difference between T_{02} and T_{03}, see text.

[b]Preferred value, see text.

Table 8. Y(nHc) values for SBS 0335–052

	T(He II)	N_e(He II) (cm^{-3})					
t^2	(K)	241	257	279	297	316	362
0.004[a]	20,020	0.2439	0.2425[b]	0.2409	0.2396	0.2382	0.2351
0.014	19,590	0.2442	0.2430	0.2413[b]	0.2400	0.2387	0.2356
0.021	19,290	0.2445	0.2433	0.2416	0.2403[b,c]	0.2390	0.2360
0.028	18,990	0.2447	0.2435	0.2419	0.2406	0.2393[b]	0.2363

[a]Minimum t^2 value, assuming that ${t_2}^2 = {t_3}^2 = 0.000$ and considering the difference between T_{02} and T_{03}, see text.

[b]Minimum χ^2 value at a given t^2.

[c]Best fit (minimum χ^2 value) for this object.

Table 9. Y Comparison

	O[a]	Y(nHc)[b] $t^2 = 0.000$	Y(nHc)[c] $t^2 \neq 0.000$	Y(+Hc)[c] $t^2 \neq 0.000$
NGC 346	1714 ± 255	.....	0.2405 ± 0.0017	0.2421 ± 0.0018
NGC 2363	1155 ± 97	0.2456 ± 0.0008	0.2424 ± 0.0035	0.2456 ± 0.0039
Haro 29	948 ± 122	0.2509 ± 0.0012	0.2388 ± 0.0040	0.2420 ± 0.0044
SBS 0335–052	392 ± 36	0.2463 ± 0.0015	0.2403 ± 0.0048	0.2450 ± 0.0060
I Zw 18	243 ± 24	0.2429 ± 0.0070	0.2350 ± 0.0072	0.2412 ± 0.0085
Y_p(sample)		0.2445 ± 0.0009[d]	0.2356 ± 0.0020[d]	0.2386 ± 0.0025[d]

[a]Oxygen abundance by mass for $t^2 \sim 0.02$, in units of 10^{-6}.

[b]Izotov & Thuan (1998); Izotov et al. (1999).

[c]This paper.

[d]Derived from the sample under the assumption that $\Delta Y/\Delta O = 3.5 \pm 0.9$ (see Paper I).

Table 10. Baryon densities for $h = 0.70$

Method	Ω_b		Source
D_p	0.035 - 0.049	(2σ)	O'Meara et al. (2001)
Li_p	0.013 - 0.026	(2σ)	Suzuki et al. (2000)
Boomerang	0.031 - 0.059	(2σ)	Netterfield et al. (2001)
CBI	0.006 - 0.060	(min-max)	Padin et al. (2001)
($z = 0$)	0.007 - 0.041	(min-max)	Fukugita et al. (1998)
($z \sim 3.0$)	0.010 - 0.060	(min-max)	Fukugita et al. (1998)
SNIa	0.018 - 0.066	(2σ)	Steigman et al. (2001)
Y_p(nHc),$t^2 = 0.000$	0.025 - 0.037	(2σ)	this paper
Y_p(nHc),$t^2 \neq 0.000$ [a]	0.011 - 0.020	(2σ)	this paper
Y_p(+Hc),$t^2 \neq 0.000$ [a]	0.012 - 0.027	(2σ)	this paper

[a]Recommended values, see text.

Fig. 1.— T_e(He II)/T_e(O III) as a function of T_e(O III) and temperature fluctuations for the case in which all the O is O^{++}. When O^+ is present higher t^2 values are expected, particularly for those objects with the highest T_e(O III) values (see Figure 2). Typical t^2 values in H II regions are in the 0.01 to 0.04 range.

Fig. 2.— T_e(O III) versus T_e(He II) showing the effect of different O^+ fractions and different total t^2 on T_e(He II). Notice that when O^+ is present there are forbidden regions that correspond to the low end of t^2 (those regions where the lines stop) because it is unphysical to assume a uniform T_e(He II) when one is already using 2 different temperatures for a given line of sight: T_e(O III) *and* T_e(O II). The T_e(O II) for the O^+ fraction is assumed to be the one derived from the photoionization models by Stasińska (1990).

Fig. 3.— Y(nHc) versus O/H diagram. Results for $t^2 = 0.000$ (Izotov & Thuan 1998; Izotov et al. 1999) are shown as open circles, the error bars are those quoted by the authors, they include the errors in the measurements of the lines, but assume no uncertainties on the determination of T_e(He II), N_e(He II), or $\tau(3889)$; results for $t^2 \neq 0.000$ (this paper) are shown as solid dots, the errors represent the uncertainties on: the intensities of the lines, T_e(He II), N_e(He II), and $\tau(3889)$; other possible systematic effects (such as the collisional contribution to the Balmer lines, or errors on the atomic physics) are not included, see text. The lines represent the best fits to the data assuming a slope of $\Delta Y/\Delta O = 3.5 \pm 0.9$, see text.

Fig. 4.— Helium, deuterium, and lithium abundances predicted by standard Big Bang nucleosynthesis computations with three light neutrino species for different values of η, the baryon to photon ratio (Thomas et al. 1994; Fiorentini et al. 1998). Also in this figure we present observational abundance determinations of these elements. The helium boxes are 1σ determinations from this work; the solid line boxes correspond to Y_p(nHc) and the dotted line boxes to Y_p(+Hc) (see Tables 9 and 10). The deuterium box is the 1σ determination by O'Meara et al. (2001) while the lithium box is the 2σ determination by Suzuki, Yoshii, & Beers (2000).

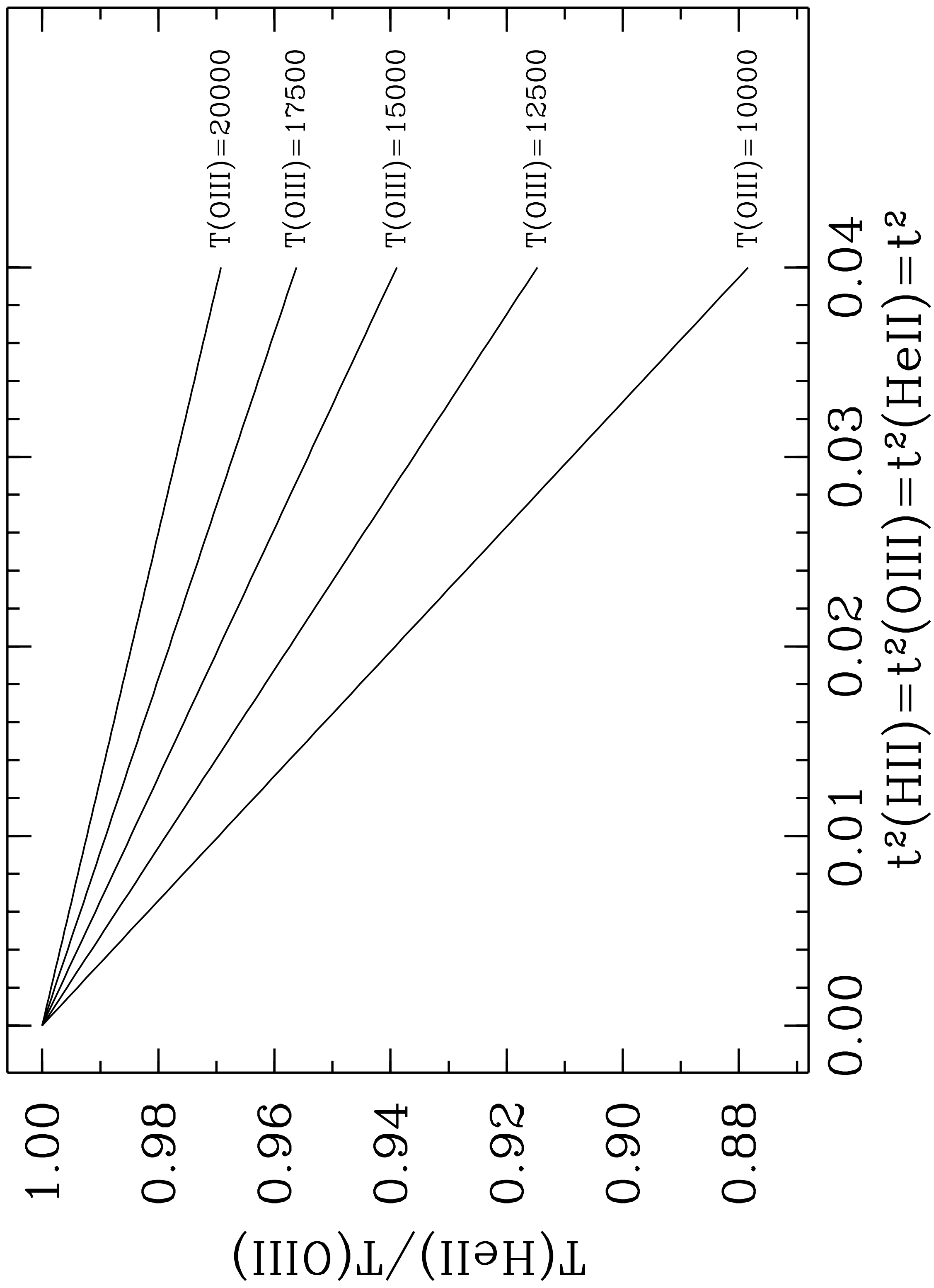
T(HeII)/T(OIII)
1.00
0.98
0.96
0.94
0.92
0.90
0.88
0.00
0.01
0.02
0.03
0.04
t²(HII)=t²(OIII)=t²(HeII)=t²
T(OIII)=20000
T(OIII)=17500
T(OIII)=15000
T(OIII)=12500
T(OIII)=10000

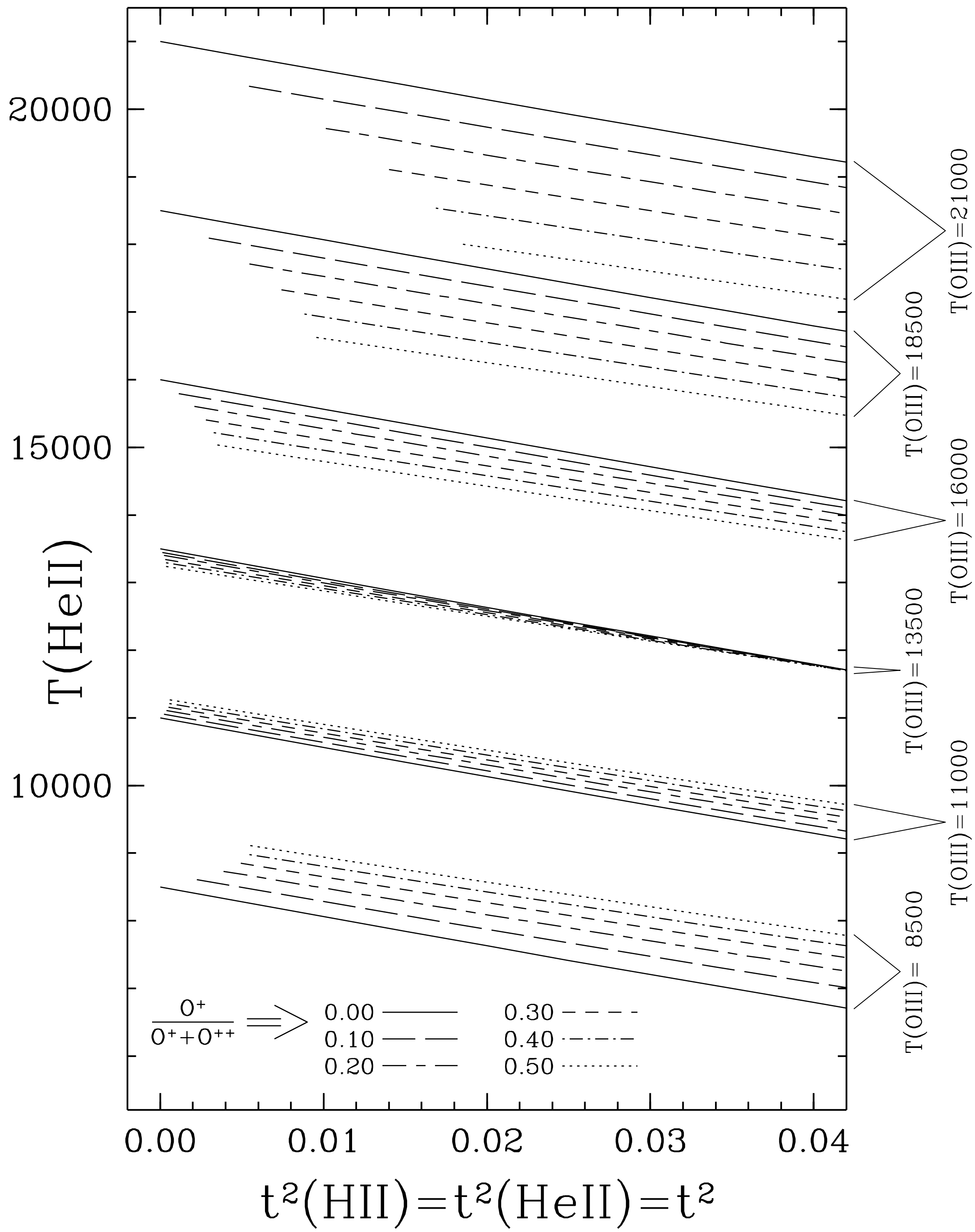
20000
15000
10000
T(HeII)
0.00
0.01
0.02
0.03
0.04
t²(HII)=t²(HeII)=t²
T(OIII)=21000
T(OIII)=18500
T(OIII)=16000
T(OIII)=13500
T(OIII)=11000
T(OIII)= 8500
O⁺ / O⁺+O⁺⁺
0.00
0.10
0.20
0.30
0.40
0.50

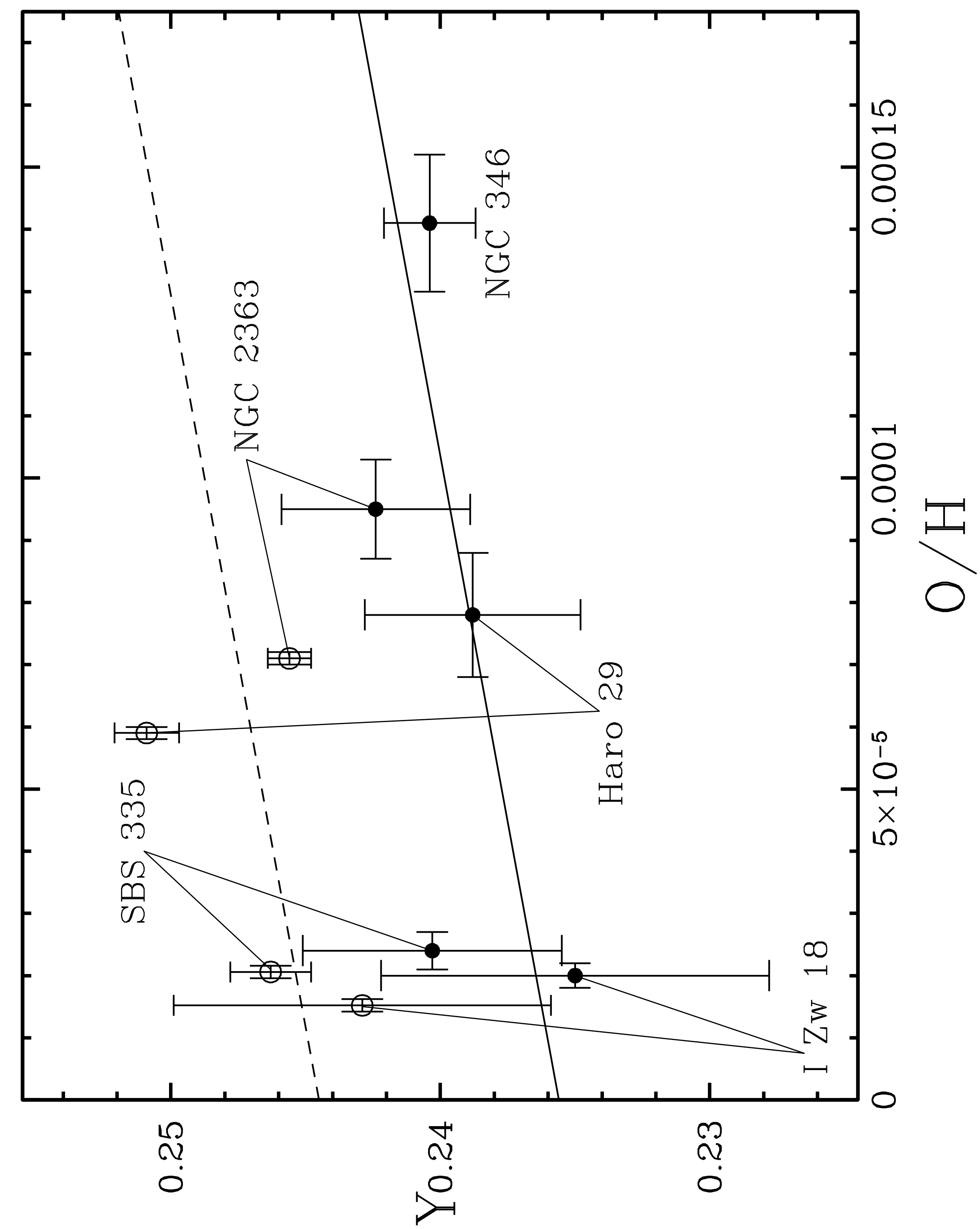
NGC 346
NGC 2363
Haro 29
SBS 335
I Zw 18
O/H
Y
0
5×10⁻⁵
0.0001
0.00015
0.25
0.24
0.23

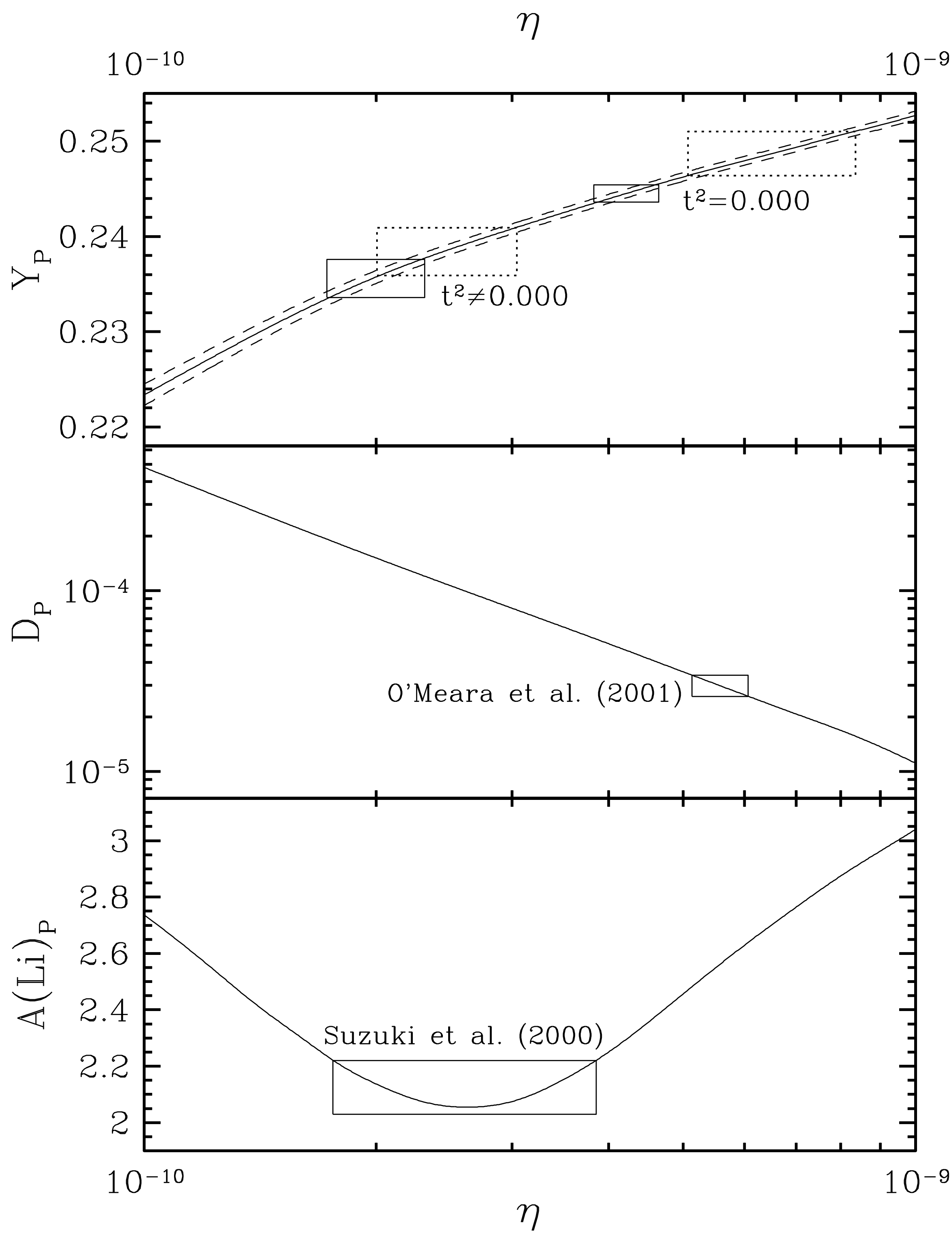
η
10^-10
10^-9
0.25
0.24
0.23
0.22
Y_P
t²=0.000
t²≠0.000
D_P
10^-4
10^-5
O'Meara et al. (2001)
A(Li)_P
3
2.8
2.6
2.4
2.2
2
Suzuki et al. (2000)
10^-10
10^-9
η